# Optimal energy management and sizing of renewable energy and battery systems in residential sectors via a stochastic MILP model

Farrokhifar, Meisam; Aghdam, Farid Hamzeh; Alahyari, Arman; Monavari, Ali; Safari, Amin

*Published in:*
Electric Power Systems Research

*DOI:*
10.1016/j.epsr.2020.106483

Electric Power Systems Research 187 (2020) 106483

Contents lists available at ScienceDirect

Electric Power Systems Research

journal homepage: www.elsevier.com/locate/epsr

# Optimal energy management and sizing of renewable energy and battery systems in residential sectors via a stochastic MILP model

Meisam Farrokhifar (Ph.D.)[a,b,*], Farid Hamzeh Aghdam[c], Arman Alahyari[a], Ali Monavari[d], Amin Safari (Ph.D.)[c]

[a] Center for Energy Science and Technology, Skolkovo Institute of Science and Technology, Moscow, Russia
[b] Faculty of Science and Engineering, University of Groningen, Groningen, The Netherlands
[c] Department of Electrical Engineering, Azarbaijan Shahid Madani University, Tabriz, Iran
[d] Department of Electrical Engineering, Roshdiyeh Higher Education Institute, Tabriz, Iran

ARTICLE INFO

*Keywords:*
Residential micro-grid
Demand response programs
Electric vehicles
Uncertainty
Mixed-integer linear programming

ABSTRACT

Energy supply through integrated renewable energy sources (RESs) and battery systems will be of higher importance for future residential sectors. Optimal energy management and sizing for the components of residential systems can enhance efficiency, self-suffiency, and meanwhile can be cost-effective by reducing investment as well as operating costs. Accordingly, this paper proposes an exhaustive optimization model for determining the capacity of RESs, namely: wind turbines and photovoltaic (PV) systems. In this study, batteries and electric vehicles (EVs) are utilized in line with other sources to capture fluctuations of RESs. To model the uncertainties of RESs, energy prices, and load demands a linearized stochastic programming framework is applied. The proposed framework involves long-term and efficient resource development alongside with short-term management and utilization of these resources for supplying the demand load. In our study, we utilize the roulette wheel mechanism (RWM) method as well as proper probability distribution functions (PDFs) to generate scenarios for all sources of uncertainties, including wind turbines, PV systems, demand, and electricity market price. The approach is verified in two different cases, including an individual home and a larger micro-grid (MG). The results of multiple numerical simulations demonstrate the effectiveness of the proposed stochastic model.

## 1. Introduction

Nowadays, with the global industrial development, the need to preserve the resources of fossil fuels for future generations, and to prevent the environmental damages caused by their burning, the alternative for providing the energy demand turn to renewable energy sources (RESs) [1]. Renewable energy development policies, which are mainly founded based on decreasing environmental concerns, expect long-term goals for developing and increasing the penetration of these resources into power systems [2]. In many parts of the world, these policies are implemented in the planning and operating phase of power systems and seem to cause a 5 to 25% increase in the share of renewable energy from total electricity production over the next decade [3]. Although RESs have numerous benefits, recent studies also have shown that the high penetration of these resources can impose new challenges both on the technical and the economic aspects, which in turn, intensifies the need to accurately assess the consequences of the full development of these resources. However, with a combination of grid optimization techniques [4] and proper planning methods [5], it is possible to have a reliable system.

Several solutions have been proposed to address these challenges, among which micro-grids (MGs) at different levels are of particular importance [6]. An MG consists of power sources and electrical loads, which commonly is connected to the conventional grid; however, it can also operate in island mode and function separately. The power sources could be small generators located in a building to handle the load for a specific time or can locally include distributed generations (DGs) to supply a wide area of a city [7]. The application of battery energy storage systems (BESSs) can support MGs during the peak demand period by returning stored excess produced energy. DGs in these systems may include numbers of RESs i.e., wind turbines and photovoltaic (PV) systems or conventional systems such as diesel generators. Nevertheless, individual applications of RESs can introduce new issues into the power system. For example, wind and solar energy resources

* Corresponding author at: Center for Energy Science and Technology, Skolkovo Institute of Science and Technology, Moscow, Russia.
*E-mail addresses:* m.farrokhi@skoltech.ru (M. Farrokhifar), farid.hamzeh@gmail.com (F.H. Aghdam), arman.alahyari@skoltech.ru (A. Alahyari), alimonavari54@gmail.com (A. Monavari), safari@azaruniv.ac.ir (A. Safari).

https://doi.org/10.1016/j.epsr.2020.106483
Received 4 July 2019; Received in revised form 1 May 2020; Accepted 17 June 2020
Available online 30 June 2020

## Nomenclature

$n$ Index for years.
$m$ Index for months of a year.
$j$ Index for days of a week; a workday: 1, a weekend: 2.
$t$ Index for hours.
$\omega$ Index for scenarios.
$N_p$ Planning period (Year).
$M$ Set for months of a year (12 months).
$J$ Set for weekdays (including a workday and a weekend).
$T$ Set for time intervals of one day (24 h).
$\Omega$ Set for examined scenarios.
$d$ Interest rate.
$\Delta(t)$ Power exchange interval (hour).
$Fix$ Share of fixed loads from the total predicted load.
$Tran$ Share of transferable loads from the total predicted load.
$Cur$ Share of curtailable loads from the total predicted load.
$\pi(m, j, \omega)$ Probability for occurrence of scenario $\omega$ in day $j$, month $m$.
$\lambda^{buy}(m, j, t, \omega)$ Forecasted price for buying energy from the upstream network ($/kWh$).
$\lambda^{sell}(t)$ Forecasted price for selling energy to the upstream network ($/kWh$).
$TNPV$ Net present value of total investment and project costs ($).
$TPV_{out}$ Net present value of total investment cost ($).
$TPV_{inc}$ Net present value of total development proceeds ($).
$C_{cap,tot}$ Total investment costs ($).
$C_{rep,tot}$ Total replacement and placement costs ($).
$C_{main,tot}$ Total maintenance costs ($).
$C_{cap,pv}$ Total investment costs of PV systems ($).
$C_{cap,ess}$ Total investment costs of energy storage systems ($).
$C_{cap,wnd}$ Total investment costs of wind units ($).
$\eta_{pv}$ The optimum capacity for PV systems ($kW$).
$\eta_{ess}$ The optimum capacity for energy storage systems ($kWh$).
$\eta_{wnd}$ The optimum capacity for wind units ($kW$).
$C_{rep,pv}$ Cost of replacing PV systems ($).
$C_{rep,ess}$ Cost of replacing energy storage systems ($).
$C_{rep,wnd}$ Cost of replacing wind units ($).
$PV^{n}_{rep,flag}$ Indicator of the time of replacement of PV systems during the planning period.
$ESS^{n}_{rep,flag}$ Indicator of the time of replacement of storage systems during the planning period.
$Wnd^{n}_{rep,flag}$ Indicator of the time of replacement of wind units during the planning period.
$C_{main,pv}$ Maintenance cost of PV systems ($).
$C_{main,ess}$ Maintenance cost of energy storage systems ($).
$C_{main,wnd}$ Maintenance cost of wind units ($).
$TC_{base}$ Total expected operating costs of the system ignoring the possibility of resource development ($).
$TC_{com}$ Total expected operating costs of the system considering the possibility of resource development ($).
$P^{buy}_{grid}(m, j, t, \omega)$ Purchased power from the upstream network ($kW$).
$P^{sell}_{grid}(m, j, t, \omega)$ Sold power to the upstream network ($kW$).
$P^{\max-buy}_{grid}$ Maximum power available for buying from upstream network ($kW$).
$P^{\max-sell}_{grid}$ Maximum power available for selling to the upstream network ($kW$).
$U^{buy}_{grid}(m, j, t, \omega)$ Indicator of the purchase status from the upstream network.
$P^{used}_{pv}(m, j, t, \omega)$ Power of the PV system consumed by the MG ($kW$).
$P^{sold}_{pv}(m, j, t, \omega)$ Power of the PV system sold to the upstream network ($kW$).
$P^{prod}_{pv}(m, j, t, \omega)$ Produced power of the PV system ($kW$).
$P^{used}_{wnd}(m, j, t, \omega)$ Power of the wind unit consumed by the MG ($kW$)
$P^{sold}_{wnd}(m, j, t, \omega)$ Power of the wind sold to the upstream network ($kW$).
$P^{prod}_{wnd}(m, j, t, \omega)$ Produced power of the wind unit ($kW$).
$P^{used}_{ess}(m, j, t, \omega)$ Power of the energy storage system consumed by the MG ($kW$).
$P^{sold}_{ess}(m, j, t, \omega)$ Power of the energy storage system sold to the upstream network ($kW$).
$P^{used}_{ev}(m, j, t, \omega)$ Power of the EV consumed by the MG ($kW$).
$P^{sold}_{ev}(m, j, t, \omega)$ Power of the EV sold to the upstream network ($kW$).
$P^{cons}_{load}(m, j, t, \omega)$ Power consumption ($kW$).
$P^{prid}_{load}(m, j, t, \omega)$ Total forecasted power consumption ($kW$).
$D^{F}_{load}(m, j, t, \omega)$ Uncontrollable power consumption ($kW$).
$D^{T-\mathrm{mod}}_{load}(m, j, t, \omega)$ Power consumption after transfer to other periods ($kW$).
$D^{T}_{load}(m, j, t, \omega)$ Power consumption to be transferred ($kW$).
$D^{C}_{load}(m, j, t, \omega)$ Residential power which can be reduced once more ($kW$).
$\rho^{T}_{load}(t, t')$ Transfer penalty ratio of 1 $kW$ from hour $t$ to hour $t'$ ($/kWh$).
$Pen^{T}_{tran}(m, j, t, \omega)$ Penalty of load transfer to another period ($).
$\rho^{C}_{load}(t)$ Curtailment penalty ratio of 1 $kW$ form consumption at hour $t$ ($/kWh$).
$Pen^{T}_{cur}(m, j, t, \omega)$ Penalty of load curtailment ($).
$U^{T}_{load}(m, j, t, t', \omega)$ Power transferred from hour $t$ to hour $t'$ ($kW$).
$IF^{\max}_{load}(t)$ Maximum power consumption transferable to hour $t$ ($kW$).
$OF^{\max}_{load}(t)$ Maximum power consumption transferable from hour $t$ ($kW$).
$P^{ch}_{ev}(m, j, t, \omega)$ Planned power to charge an EV ($kW$).
$P^{dis}_{ev}(m, j, t, \omega)$ Planned power to discharge an EV ($kW$).
$P^{ch}_{ess}(m, j, t, \omega)$ Planned power to charge the energy storage system ($kW$).
$P^{dis}_{ess}(m, j, t, \omega)$ Planned power to discharge the energy storage system ($kW$).
$DE_{ess}$ Discharging efficiency of the energy storage system.
$DE_{ev}$ Discharging efficiency of the EV.
$CE_{ess}$ Charging efficiency of the energy storage system.
$CE_{ev}$ Charging efficiency of the EV.
$\eta^{\max}_{ess}$ Maximum expandable capacity of energy storage systems ($kWh$).
$\eta^{\max}_{pv}$ Maximum expandable capacity of PV systems ($kW$).
$\eta^{\max}_{wnd}$ Maximum expandable capacity of wind units ($kW$).
$U_{ev}(m, j, t, \omega)$ Indicator for the status of charging or discharging of the EV.
$U_{grid}(m, j, t, \omega)$ Indicator for the status of power supply form the grid.
$U_{ess}(m, j, t, \omega)$ Indicator for the status of charging or discharging of the energy storage system.
$CR^{\max}_{ess}$ Maximum charging rate of the energy storage system ($kW/h$).
$DR^{\max}_{ess}$ Maximum discharging rate of the energy storage system ($kW/h$).
$CR^{\max}_{ev}$ Maximum charging rate of the EV ($kW/h$).
$DR^{\max}_{ev}$ Maximum discharging rate of the EV ($kW/h$).
$SOE_{ess}(m, j, t, \omega)$ Remaining energy level of the energy storage system ($kWh$).
$SOE_{ev}(m, j, t, t', \omega)$ Remaining energy level of the EV ($kWh$).
$SOE^{ini}_{ess}$ Initial energy level of the energy storage system ($kWh$).
$SOE^{ini}_{ev}$ Initial energy level of the EV ($kWh$).
$SOE^{\max}_{ess}$ Maximum energy level of the energy storage system ($kWh$).
$SOE^{\min}_{ess}$ Minimum energy level of the energy storage system ($kWh$).
$SOE^{\max}_{ev}$ Maximum energy level of the EV ($kWh$).
$SOE^{\min}_{ev}$ Minimum energy level of the EV ($kWh$).
$T_a$ Time of connecting the EV to the MG.
$T_d$ Time of disconnecting the EV from the MG.

have an alternating nature and are highly dependent on environmental conditions. Independent use of PV systems or wind turbines will increase the size and cost of the system [8]. In the case of RESs, batteries are the most common systems used as energy storage systems [9]. Therefore, an energy storage system such a battery should be operated with RESs [10] to reduce power fluctuations. The optimal sizing of a hybrid RES-based system could maximize the self-sufficiency of the MG [11]. Besides, proper scheduling of these systems can greatly reduce the operating costs, purchased energy from the upstream network [8], and amount of energy loss [12].

Recently, electric vehicles (EVs) as potential elements of MGs are increasingly welcomed by consumers. The main advantages of EVs compared to conventional cars are less environmental pollution, higher efficiency, less noise, and more comfortable charging facilities [13]. In addition, the EVs are widely operated in the presence of RESs [14] and can also inject power into the grid [15]. Due to the role of EVs in distribution networks, numerous research works have been done in the area of these grids and MG design in the presence of EVs [16]. A two-step linear programming approach was proposed in [17] to determine the optimal location and operation of EV charging stations in distribution networks. Clairand et al. [18] investigated the generation planning problem in diesel-based MGs with RESs, considering supplying of EVs and cooking purposes and reducing environmental impact. A comprehensive approach for planning, development, and operation of MGs with BESSs as well as EVs was presented in [19]. The authors in [15] applied a two-stage model to build parking lots in the distribution network, which aims to minimize cost, reliability, and voltage deviations. In the first stage of this model, the behavior of EVs is optimized by considering their interactions with the market. In the second stage, the problem of parking lot placement is solved by considering the network constraints. Moradijoz et al. [20] provided a multi-objective dynamic bi-level model for distribution network planning. Besides, the authors considered grid-connected EV parking lots in their model to improve the flexibility of the system.

Uncertainties have become one of the indisputable concepts in recent literature. Various uncertainty sources were investigated in [21] through a probabilistic approach for BESSs sizing to support the integration of PV systems in distribution grids. The authors in [22] provided a method for planning and development of distribution networks integrating RESs and demand response programs as planning options for the transition to RES-based distribution networks. In this reference, demand response is assumed to be activated by real-time price signals and the problem is implemented in the form of a bi-level dynamic model with the goal of minimizing the technical costs and costs associated with the emission of greenhouse gases. Uncertainties in the problem include the uncertainties of RESs and the uncertainties associated with the sensitivities of costumers to the electricity prices. A chance-constrained information gap decision model for MG expansion planning was proposed in [23]. In this reference, two types of uncertainties, as random and non-random uncertainties, were considered. The main objective is determining the best type of renewables, optimal sizing, and their installation time in the MG. The authors in [24] proposed a probabilistic multi-objective model for planning active distribution networks in the presence of demand response programs. Uncertainties about solar radiance, load levels, and load growth rates in the future are modeled by probability density function (PDF). The proposed model simultaneously minimizes operating costs and energy losses on the lines from the perspective of the distribution network operator, taking into account demand response programs and active network management (i.e., such as voltage control patterns and power factor). In fact, the proposed model determines the level of penetration of solar panels in the network according to the stated objectives.

The problem of optimal utilization and control of MGs in various studies has been extensively investigated, research on the development and long-term planning of MGs is also of interest. A method for developing and determining the optimal capacity of solar and wind resources in a hybrid MG was presented in [8]. In this reference, data on solar irradiance, wind speed, and ambient temperature in the state of Texas have been used to test the effectiveness of the proposed algorithm. Also, the effect of demand response programs on increasing productivity and optimal design has been studied. Nevertheless, the authors did not consider vehicle-to-grid capabilities in their work. A techno-economic optimization model using the particle swarm optimization (PSO) algorithm was performed to determine the optimum size of PV, battery, and other components of a residential MG in [25]. However, evolutionary methods like PSO do not guarantee to reach a globally optimal solution. In [26], a method for the development and planning of advanced MGs with the capability of managing energy storage systems, EVs and responsive loads was proposed to improve the security issues at the time of islanded operation. A framework for the utilization of DGs in the distribution network for planning and designing robust MGs was presented in [27]. The authors in this study tried to optimally enhance the reliability and economic efficiency of the MG. The proposed model was solved by multi-agent systems and the PSO method. The authors in [28] proposed a multi-objective optimization method to evaluate the optimal operation and planning of DGs in MG networks. Also, the authors introduced an index for evaluating the security of the system based on the capability of the power system in restoring to a new operating point after experiencing an unwanted event. In [5], the problem of planning and designing hybrid MGs was addressed, considering the emission limits and the costs associated with the lifetime of RESs. In this study, it was shown that the combination of diesel and renewable units, compared with the use of diesel units alone, leads to lower levels of pollution and lower net costs. However, only wind units were considered among RESs in this reference, and other options for these sources were ignored. Optimal allocation of DGs for optimal utilizing an MG was presented in [29]. In this study, sensitivity analysis and the PSO algorithm were used to carry out cost-benefit analysis and to ensure reliability criteria at different load points. The authors in [30] evaluated the generation planning in an MG, taking into account the emission constraints. In this reference, the genetic algorithm was used to determine the optimal allocations of wind and solar resources. In [31], a bi-level algorithm was proposed for the optimal planning and design of an MG using the combined heat and power (CHP) units, considering the issue of reducing carbon dioxide emissions. In [32], the formation of multiple MGs system was studied with the aim of improving the recovery operation in the distribution network. In this reference, the problem was formulated as a linear optimization model.

In this paper, the problem of determining the optimum capacity of energy storage and RESs, including wind units and PV systems in a residential MG, considering the possibility of utilizing demand response programs and EVs, is investigated. To the best knowledge of the authors, none of the reviewed literature has considered a comprehensive study on the development of hybrid MGs. In order to overcome the shortcomings of the previous works, we try to completely address the planning problem of hybrid MGs. Short-term energy management in the planning process is taken into account to have a better perspective of the overall operating and planning costs to make better decisions. Due to the rapid development of EV technologies, we consider the vehicle-to-grid option in the planning horizon. Also, we model the main sources of uncertainties in the planning problem. Besides, demand response programs as one of the most important and efficient tools of smart grids are contemplated in this work. A thorough numerical study is done to demonstrate the effectiveness of the proposed method. In conclusion, the contributions of the paper are as follows.

- A Comprehensive framework for designing and developing RESs and BESSs in a residential MG, considering various uncertainties.
- Performing day-ahead energy management in the planning process for estimating the operating costs in different conditions of planning and better decision-making.
- Scenario-based stochastic modeling of RESs including wind and PV systems, demand levels, price signals, and EVs in the process of planning the MG.
- Considering EVs, vehicle-to-grid capability, demand response programs, and BESSs capabilities in the planning process.

The remainder of this paper is organized as follows. In Section 2, the proposed model is described to determine the optimal capacity of RESs and energy storage. Also, demand response programs and EV utilization are investigated in this section. In Section 3, by performing multiple simulations, the proposed method is discussed in detail. Finally, in Section 4, a general conclusion from the findings of research and suggestions for future work is presented.

## 2. System modeling and problem formulation

As mentioned previously, the rapid development of smart grid concepts and technologies such as RESs, EVs, and MGs, the power consumption patterns as well as the structure of electrical distribution networks have significantly changed. The design of a hybrid renewable energy system (HRES) with the use of various types of wind, solar, and storage technologies is more efficient than traditional methods of utilizing these resources. In this section, modeling of the problem of determining the optimum capacity of energy storage and RESs in a residential MG, considering the possibility of using demand response programs, is investigated.

### 2.1. Proposed framework

The proposed framework for efficient resource development, coupled with long-term planning of the components of the system, involves the management and utilization of these resources for consumption in the short-term operation. Using appropriate PDFs and scenario production methods, consumption values in the MG, purchasing prices from the upstream network, and the production of wind turbines and PV systems are modeled. The roulette wheel mechanism (RWM) is also used to derive scenarios.

The optimization process is done in two stages. In the first stage, decisions will be made on uncertain variables, and in the second stage, according to each of the scenarios, the remaining variables will be determined. In other words, the first stage will be at the time of decision-making to determine the optimal resource capacity, and the second stage will be based on the realization of each of the relevant scenarios at the time of operation, including the constraints of the problem.

Also, to reduce the system operating costs and increase its flexibility against the existing uncertainties, demand response programs will be contemplated. The studied MG is able to exchange energy with the upstream network.

Although the development of electric transportation systems and EVs increase power consumption, they could create more flexibility on the demand side by adding the ability of intended charging and discharging. Hence, in the proposed model, the MG operator can use EVs connected to the grid to manage uncertainties and more profitability.

The framework of the HRES is explained in Fig. 1. In this structure, RESs produce energy along with traditional power sources; meanwhile, BESSs and PVs are employed for energy exchange. It is worth mentioning that, residential sectors include two types of load namely controllable and uncontrollable. For controllable loads, it is possible to reduce consumption (with considering a penalty value for the reduction in their welfare) or to change the consumption time from peak times with higher prices to non-peak periods with lower prices or periods in which RESs generate at their maximum value.

Also, the concept of net present value (NPV) is used to evaluate plans and to economize the feasibility of long-term development plans. Due to the high efficiency of linear models, modeling and formulation of the proposed model are implemented in the form of a mixed-integer linear programming (MILP) problem. The output of the optimization problem determines the capacity of wind, solar, and BESSs. Besides, the optimal operation of the MG, including scheduling of the controllable loads, the amount of charge and discharge of BESSs, and the intelligent management of EVs during the planning period will be determined for different scenarios and for various working conditions. The flowchart of the proposed algorithm is presented in Fig. 2. In order to model the uncertainties related to the production of renewable wind and solar energy resources, purchase prices from the upstream network and the amount of consumption in the studied microgrid, a framework based on

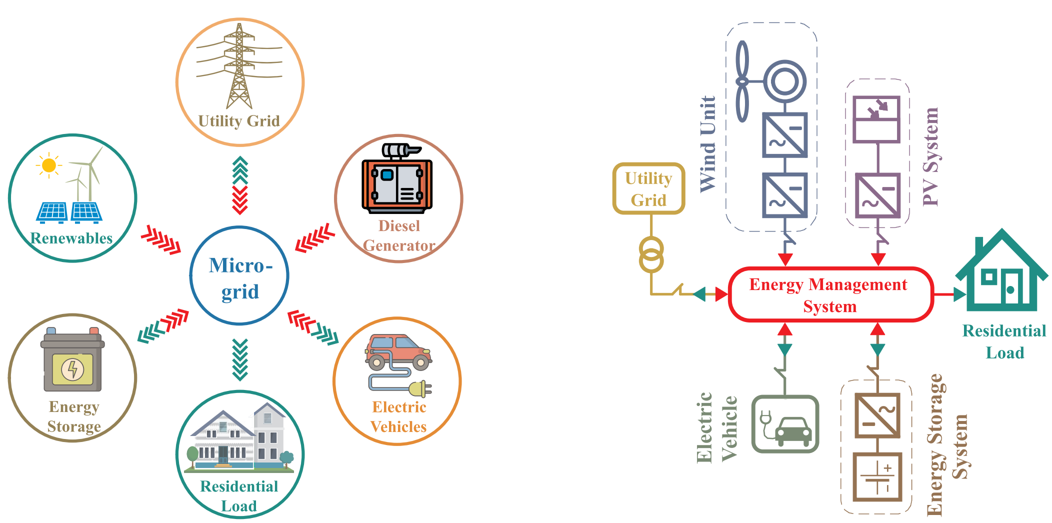


(a) Structure of a micro-grid.

(b) Single line diagram for a residential load.

**Fig. 1.** Framework of the hybrid renewable energy systems.

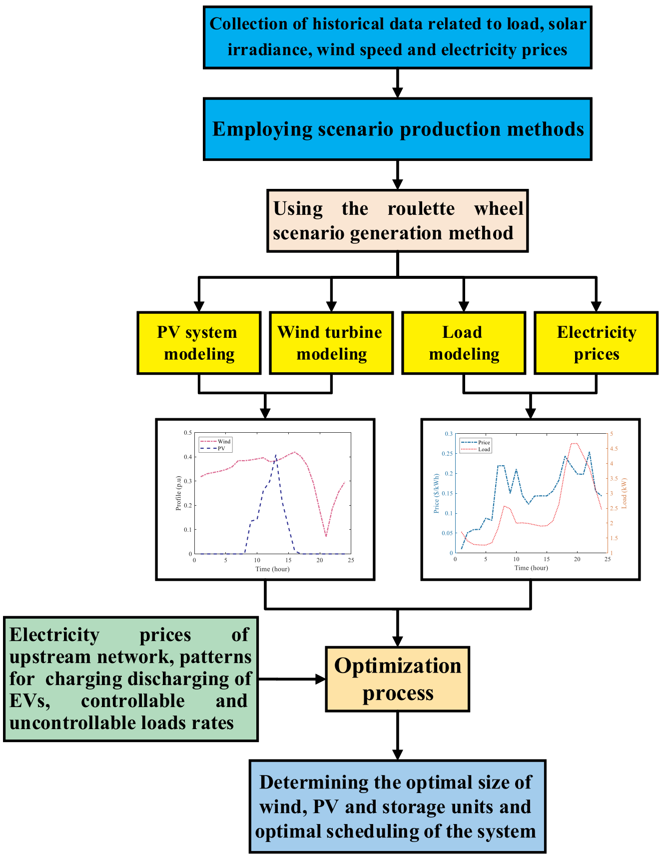


**Fig. 2.** Proposed optimization scheme.

random programming is presented. In this method, first, data for wind generation, solar irradiance, load, and electricity price for a specific area is collected. By using this data, PDFs are fitted for the variables with uncertainty and employing an RWM, scenarios for the planning purposes are generated. The optimization process is done in two stages. In the first stage, decisions regarding uncertainty variables will be made, and in the second stage, the remaining variables will be determined according to the realization of each of the scenarios. In other words, the first stage will be at the time of decision-making to determine the optimal capacity of resources (here-and-now stage), and the second stage will be done depending on the realization of each of the relevant scenarios at the time of operation and will include constraints and limitations (wait-and-see stage). The results indicate the optimum planning values for PV, wind, and battery systems.

### 2.2. Scenario generation

For scenario generation, the information and historical data related to the past few years of the system are considered. In the next step, the probability distribution function (PDF) of prediction error for uncertain parameters is extracted and discretized in different levels, as shown in Fig. 3a. According to this figure, each probability level of the error is demonstrated with $\alpha$ and each interval represents one standard deviation error ($\beta$). Then, the RWM is used to generate the scenarios [33]. In establishing the roulette wheel, the higher the probability of parameter, the more space it. For the mentioned levels, the produced roulette wheel is presented in Fig. 3b. In this mechanism, a random number is generated in the range of zero and one. This number is in one of the specified intervals on the roulette wheel, which is related to the level of parameter prediction error. The aforementioned probability level is selected for the desired scenario. It is obvious a scenario with a smaller level of prediction error gets a higher selection chance in the RWM. By combining all the errors related to each uncertainty source, the first scenario is generated. Later, by multiplying the probabilities of uncertainty parameters, the probability of the whole scenario is obtained. Finally, different scenarios are generated utilizing the mentioned mechanism.

### 2.3. Problem modeling, objective function and problem constraints

The problem is formulated in the form of a stochastic MILP model in order to consider the uncertainties associated with the problem. The objective function could be formulated as (1). In this regard, minimizing the net present value of the total investment and operating costs of the project is the goal of optimization.

$$\min:\ TNPV = TPV_{out} - TPV_{inc} \tag{1}$$

In (1), the minimization of the $TNPV$, is obtained by minimizing investment costs $TPV_{out}$ and maximizing the revenue from resource development $TPV_{inc}$. The investment cost $TPV_{out}$ includes the total cost of developing, replacing and maintaining new wind, solar, and energy storage resources during the planning period, which is illustrated in (2).

$$TPV_{out} = C_{cap,tot} + C_{rep,tot} + C_{main,tot} \tag{2}$$

The total cost of development, replacement and maintenance of resources are calculated by (3) to (5). In these equations, the NPV concept is used to evaluate and economical feasibility during the planning period.

$$C_{cap,tot} = C_{cap,pv} \times \eta_{pv} + C_{cap,wnd} \times \eta_{wnd} + C_{cap,ess} \times \eta_{ess} \tag{3}$$

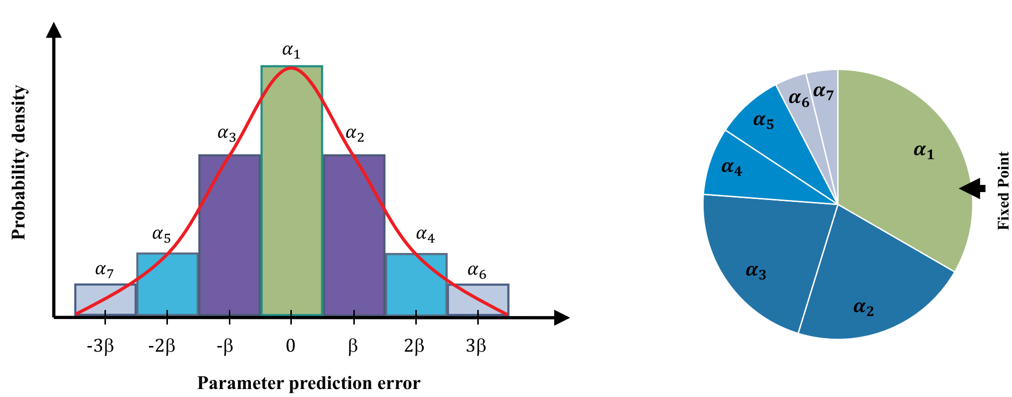


(a) Conversion of the PDF to discrete levels. (b) Generated roulette wheel with seven pieces.

**Fig. 3.** Scenario generation process.

$$C_{rep,tot} = \sum_{n=1}^{Np} [\frac{PV_{rep,flag}^{n} \times C_{rep,pv} \times \eta_{pv}}{(1+d)^n} + \frac{ESS_{rep,flag}^{n} \times C_{rep,ess} \times \eta_{ess}}{(1+d)^n} + \frac{Wnd_{rep,flag}^{n} \times C_{rep,wnd} \times \eta_{wnd}}{(1+d)^n}] \quad (4)$$

$$C_{main,tot} = \sum_{n=1}^{Np} \left[\frac{C_{main,pv} \times \eta_{pv} + C_{main,ess} \times \eta_{ess} + C_{main,wnd} \times \eta_{wnd}}{(1+d)^n}\right] \quad (5)$$

To calculate the expected revenue from resource development $TPV_{inc}$, according to (6), the difference of NPV in operating of the system costs during the planning period, considering and neglecting development capability, will be calculated. In other words, $TPV_{inc}$ represents a reduction in operating costs by resource development.

$$TPV_{inc} = \sum_{n=1}^{Np} \frac{(TC_{base} - TC_{com})}{(1+d)^n} \quad (6)$$

Operating costs of the system are formulated in the planning period using (7), which is the difference between the energy costs of the upstream network and the revenue generated by selling energy produced by the MG resources to the upstream network. To calculate the base state operating cost ($TC_{base}$), the initial installed capacity of the MG is considered. If there is no initial installed capacity of these resources, then the MG revenue from energy selling to the upstream grid equals zero.

$$TC_{com} = \sum_{n=1}^{Np} \sum_{m \in M} \sum_{j \in J} \sum_{\omega \in \Omega} \pi(m,j,\omega) \left[\sum_{t \in T} \Delta(t) \left( P_{grid}^{buy}(m,j,t,\omega) \times \lambda^{buy}(m,j,t,\omega) - P_{grid}^{sell}(m,j,t,\omega) \times \lambda^{sell}(t) \right)\right] \quad (7)$$

The power balance constraint of the MG is shown in (8). This relationship states that the sum of the power purchased from the upstream network ($P_{grid}^{buy}$), solar power generation ($P_{pv}^{used}$), EV power ($P_{ev}^{used}$), wind turbine power ($P_{wnd}^{used}$) and energy storage power injected to the MG ($P_{ess}^{used}$) will be used for charging the energy storage ($P_{ess}^{ch}$) and charging the EV ($P_{ev}^{ch}$) and power consumption of the loads ($P_{load}$).

$$P_{grid}^{buy}(m,j,t,\omega) + P_{wnd}^{used}(m,j,t,\omega) + P_{pv}^{used}(m,j,t,\omega) + P_{ev}^{used}(m,j,t,\omega) + P_{ess}^{used}(m,j,t,\omega) = P_{load}(m,j,t,\omega) + P_{ev}^{ch}(m,j,t,\omega) + P_{ess}^{ch}(m,j,t,\omega) \quad \forall m \in M, \forall j \in J, \forall t \in T, \forall \omega \in \Omega \quad (8)$$

The constraints and scheduling of the grid-connected BESS are modeled by (9) to (18).

$$P_{ess}^{used}(m,j,t,\omega) + P_{ess}^{sold}(m,j,t,\omega) = P_{ess}^{dis}(m,j,t,\omega) \times DE_{ess} \quad \forall m \in M, \forall j \in J, \forall t \in T, \forall \omega \in \Omega \quad (9)$$

$$P_{ess}^{ch}(m,j,t,\omega) \le \eta_{ess}^{\max} \times U_{ess}(m,j,t,\omega) \quad \forall m \in M, \forall j \in J, \forall t \in T, \forall \omega \in \Omega \quad (10)$$

$$P_{ess}^{dis}(m,j,t,\omega) \le (1-\eta_{ess}^{\max}) \times U_{ess}(m,j,t,\omega) \quad \forall m \in M, \forall j \in J, \forall t \in T, \forall \omega \in \Omega \quad (11)$$

$$P_{ess}^{ch}(m,j,t,\omega) \le CR_{ess}^{\max} \times \eta_{ess} \quad \forall m \in M, \forall j \in J, \forall t \in T, \forall \omega \in \Omega \quad (12)$$

$$P_{ess}^{dis}(m,j,t,\omega) \le DR_{ess}^{\max} \times \eta_{ess} \quad \forall m \in M, \forall j \in J, \forall t \in T, \forall \omega \in \Omega \quad (13)$$

$$SOE_{ess}(m,j,t,\omega) = SOE_{ess}(m,j,t-1,\omega) + CE_{ess} \times P_{ess}^{ch}(m,j,t,\omega) - P_{ess}^{dis}(m,j,t,\omega) \quad \forall m \in M, \forall j \in J, \forall t > 1, \forall \omega \in \Omega \quad (14)$$

$$SOE_{ess}(m,j,t,\omega) = SOE_{ess}^{ini} \times \eta_{ess} \quad \forall m \in M, \forall j \in J, \forall t = 1, \forall \omega \in \Omega \quad (15)$$

$$SOE_{ess}(m,j,t,\omega) \le SOE_{ess}^{\max} \times \eta_{ess} \quad \forall m \in M, \forall j \in J, \forall t \in T, \forall \omega \in \Omega \quad (16)$$

$$SOE_{ess}(m,j,t,\omega) \ge SOE_{ess}^{\min} \times \eta_{ess} \quad \forall m \in M, \forall j \in J, \forall t \in T, \forall \omega \in \Omega \quad (17)$$

$$\eta_{ess} \le \eta_{ess}^{\max} \quad (18)$$

Eq. (9) states that the discharged power from the storage device ($P_{ess}^{dis}$) with respect to the discharge efficiency of this unit ($DE_{ess}$) is used for internal use of the MG ($P_{ess}^{used}$) and selling to the upstream network ($P_{ess}^{sold}$). Relations (10) and (11), show amounts of charging and discharging of the storage device with respect to the maximum capacity allowed for storage development ($\eta_{ess}^{\max}$) and how to operate in the states of charging or discharging of this unit ($U_{ess}$). Eqs. (12) and (13) are also related to the maximum charge ($CR_{ess}^{\max}$) and discharge ($DR_{ess}^{\max}$) rates. Eq. (14) describes state of energy ($SOE$) of the energy storage over the scheduling horizon with respect to the charge and discharge rates. Eq. (15) also describes the initial SOE of the device and finally (16), (17) and (18) demonstrate the maximum and minimum charging level allowed for the storage device and the available capacity for development, respectively.

Eqs. (19) to (27) are used to model constraints and scheduling of the EVs at times of that they are connected to the MG ($t \in [T_a \, T_d]$).

$$P_{ev}^{used}(m,j,t,\omega) + P_{ev}^{sold}(m,j,t,\omega) = P_{ev}^{dis}(m,j,t,\omega) \times DE_{ess} \quad \forall m \in M, \forall j \in J, \forall \omega \in \Omega, \forall t \in [T_a \, T_d] \quad (19)$$

$$P_{ev}^{ch}(m,j,t,\omega) \le CR_{ev}^{\max} \times U_{ev}(m,j,t,\omega) \quad \forall m \in M, \forall j \in J, \forall \omega \in \Omega, \forall t \in [T_a \, T_d] \quad (20)$$

$$P_{ev}^{dis}(m,j,t,\omega) \le DR_{ev}^{\max} \times (1 - U_{ev}(m,j,t,\omega)) \quad \forall m \in M, \forall j \in J, \forall \omega \in \Omega, \forall t \in [T_a \, T_d] \quad (21)$$

$$SOE_{ev}(m,j,t,\omega) = SOE_{ev}(m,j,t-1,\omega) + CE_{ev} \times P_{ev}^{ch}(m,j,t,\omega) - P_{ev}^{dis}(m,j,t,\omega) \quad \forall m \in M, \forall j \in J, \forall \omega \in \Omega, \forall t \in (T_a \, T_d] \quad (22)$$

$$SOE_{ev}(m,j,t,\omega) = SOE_{ev}^{ini} \quad \forall m \in M, \forall j \in J, \forall \omega \in \Omega, \forall t = T_a \quad (23)$$

$$SOE_{ev}(m,j,t,\omega) \le SOE_{ev}^{\max} \quad \forall m \in M, \forall j \in J, \forall \omega \in \Omega, \forall t \in [T_a \, T_d] \quad (24)$$

$$SOE_{ev}(m,j,t,\omega) \ge SOE_{ev}^{\min} \quad \forall m \in M, \forall j \in J, \forall \omega \in \Omega, \forall t \in [T_a \, T_d] \quad (25)$$

$$SOE_{ev}(m,j,t,\omega) = SOE_{ev}^{\max} \quad \forall m \in M, \forall j \in J, \forall \omega \in \Omega, \forall t = T_d \quad (26)$$

$$SOE_{ev}(m,j,t,\omega) = P_{ev}^{used}(m,j,t,\omega) = P_{ev}^{sold}(m,j,t,\omega) = P_{ev}^{ch}(m,j,t,\omega) = P_{ev}^{dis}(m,j,t,\omega) = 0 \quad \forall m \in M, \forall j \in J, \forall \omega \in \Omega, \forall t \notin [T_a \, T_d] \quad (27)$$

Eq. (19) states that the discharged power of the EV ($P_{ev}^{dis}$), will be used for internal use of the MG ($P_{ev}^{used}$) and selling to the upstream network ($P_{ev}^{sold}$). Relations (20) and (21) limit the amount of charge and discharge of the EV according to the maximum charge ($CR_{ev}^{\max}$) and discharge rates ($DR_{ev}^{\max}$) of the vehicle. Relation (22) models the energy level of an EV ($SOE_{ev}$) during the scheduling period and Eq. (23) also determines the initial energy level of the EV. Furthermore, relations (24) and (25) also indicate limits of the maximum and minimum permitted energy levels for the EV. Eq. (26) also determines the final energy level EV at the end of the last hour of connecting to the grid. Finally, Eq. (27) also states that at times when the EV is not connected to the grid, its participation in the network operation is zero.

Eqs. (28) to (29) and (30) to (31) are used to model the production constraints of PV panels and wind turbines respectively. Relations (28) and (30) show that the PV and wind power generation capacities in each scenario are used for internal consumption of the MG (for charging the storage device or EV) or for selling to the upstream grid. Eqs. (29) and (31) also determine the respective limits for the development of PV and wind units in the MG.

$$P_{pv}^{used}(m, j, t, \omega) + P_{pv}^{sold}(m, j, t, \omega) = P_{pv}^{prod}(m, j, t, \omega) \quad \forall\, m \in M, \;\; \forall\, j \in J, \;\; \forall\, \omega \in \Omega, \;\; \forall\, t \in T \tag{28}$$

$$\eta_{pv} \le \eta_{pv}^{\max} \tag{29}$$

$$P_{wnd}^{used}(m, j, t, \omega) + P_{wnd}^{sold}(m, j, t, \omega) = P_{wnd}^{prod}(m, j, t, \omega) \quad \forall\, m \in M, \;\; \forall\, j \in J, \;\; \forall\, \omega \in \Omega, \;\; \forall\, t \in T \tag{30}$$

$$\eta_{wnd} \le \eta_{wnd}^{\max} \tag{31}$$

Also, (32) to (34), model the limits of the power purchased and sold to the network. The total power sold to the network by solar, wind, energy storage, and EV sources is reported with (32). As well, in (33) and (34), the maximum exchangeable power with the upstream network is modeled.

$$P_{grid}^{sell}(m, j, t, \omega) = P_{ess}^{sold}(m, j, t, \omega) + P_{pv}^{sold}(m, j, t, \omega) + P_{wnd}^{sold}(m, j, t, \omega) + P_{ev}^{sold}(m, j, t, \omega) \quad \forall\, m \in M, \;\; \forall\, j \in J, \;\; \forall\, \omega \in \Omega, \;\; \forall\, t \in T \tag{32}$$

$$P_{grid}^{sell}(m, j, t, \omega) \le P_{grid}^{\max-sell} \times U_{grid}(m, j, t, \omega) \quad \forall\, m \in M, \;\; \forall\, j \in J, \;\; \forall\, \omega \in \Omega, \;\; \forall\, t \in T \tag{33}$$

$$P_{grid}^{buy}(m, j, t, \omega) \le P_{grid}^{\max-buy} \times (1 - U_{grid}(m, j, t, \omega)) \quad \forall\, m \in M, \;\; \forall\, j \in J, \;\; \forall\, \omega \in \Omega, \;\; \forall\, t \in T \tag{34}$$

Eqs. (35) to (44) are also used to model the implementation of demand response programs in the MG.

$$D_{load}^{F}(m, j, t, \omega) = Fix \times P_{load}^{prid}(m, j, t, \omega) \quad \forall\, m \in M, \;\; \forall\, j \in J, \;\; \forall\, \omega \in \Omega, \;\; \forall\, t \in T \tag{35}$$

$$D_{load}^{T}(m, j, t, \omega) = Tran \times P_{load}^{prid}(m, j, t, \omega) \quad \forall\, m \in M, \;\; \forall\, j \in J, \;\; \forall\, \omega \in \Omega, \;\; \forall\, t \in T \tag{36}$$

$$D_{load}^{C}(m, j, t, \omega) = Cur \times P_{load}^{prid}(m, j, t, \omega) \quad \forall\, m \in M, \;\; \forall\, j \in J, \;\; \forall\, \omega \in \Omega, \;\; \forall\, t \in T \tag{37}$$

$$\sum_{t' \in T} U_{load}^{T}(m, j, t', t, \omega) \le IF_{load}^{\max}(t) \quad \forall\, m \in M, \;\; \forall\, j \in J, \;\; \forall\, \omega \in \Omega, \;\; \forall\, t \in T \tag{38}$$

$$\sum_{t' \in T} U_{load}^{T}(m, j, t, t', \omega) \le OF_{load}^{\max}(t) \quad \forall\, m \in M, \;\; \forall\, j \in J, \;\; \forall\, \omega \in \Omega, \;\; \forall\, t \in T \tag{39}$$

$$\sum_{t \in T} \sum_{t' \in T} U_{load}^{T}(m, j, t, t', \omega) = \sum_{t \in T} \sum_{t' \in T} U_{load}^{T}(m, j, t', t, \omega) \quad \forall\, m \in M, \;\; \forall\, j \in J, \;\; \forall\, \omega \in \Omega, \;\; \forall\, t \in T \tag{40}$$

$$D_{load}^{T-mod}(m, j, t, \omega) = D_{load}^{T}(m, j, t, \omega) + \sum_{t' \in T} [U_{load}^{T}(m, j, t', t, \omega) - U_{load}^{T}(m, j, t, t', \omega)] \quad \forall\, m \in M, \;\; \forall\, j \in J, \;\; \forall\, \omega \in \Omega, \;\; \forall\, t \in T \tag{41}$$

$$P_{load}^{cons}(m, j, t, \omega) = D_{load}^{T-mod}(m, j, t, \omega) + D_{load}^{F}(m, j, t, \omega) + D_{load}^{C}(m, j, t, \omega) \quad \forall\, m \in M, \;\; \forall\, j \in J, \;\; \forall\, \omega \in \Omega, \;\; \forall\, t \in T \tag{42}$$

$$Pen_{tran}^{T}(m, j, t, \omega) = \sum_{t' \in T} [\rho_{load}^{T}(t, t') \times \Delta(t) \times U_{load}^{T}(m, j, t, t', \omega)] \quad \forall\, m \in M, \forall\, j \in J, \forall\, \omega \in \Omega, \forall\, t \in T \tag{43}$$

$$Pen_{cur}^{T}(m, j, t, \omega) = \rho_{load}^{C}(t) \times \Delta(t) \times (P_{load}^{prid}(m, j, t, \omega) - D_{load}^{C}(m, j, t, \omega)) \quad \forall\, m \in M, \;\; \forall\, j \in J, \;\; \forall\, \omega \in \Omega, \;\; \forall\, t \in T \tag{44}$$

It is assumed that loads of the MG are divided into three categories of fixed, transferable, and curtailable loads. According to (35) to (37), the share of each load type is defined as a percentage of the total predicted load. Eqs. (38) and (39), determine the limit for the maximum input and output load power to each of the time intervals. Relation (40) also states that the sum of all outgoing power from each programming period equals to the sum of the inputs. The modified hourly transferable power after the shifting of the load to another period is shown in (41) and the power consumption at each hour after the shifting or reduction of the load is modeled in terms of (42). Finally, (43) and (44) indicate the penalty resulting from a decrease in the welfare in each hour as a result of load transfer to another period and load curtailment. These penalties should be added to (7).

## 3. Simulation and results

In this section, the presented formulations to determine the optimal capacity of RESs and batteries are examined using numerical case studies. The performance of the proposed model is investigated in two different cases. In the first case, the test system is an individual home that has the capability to install RESs as well as the battery on its roof and it has a small load and electricity consumption. Also, in the second

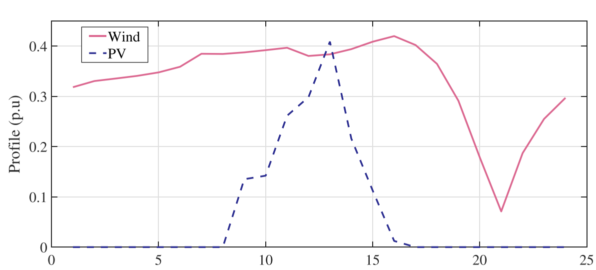


(a) PV system and wind turbine generations.

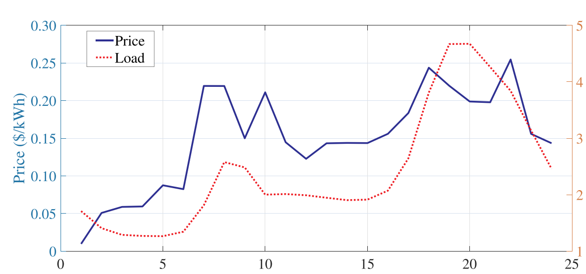


(b) Load curve and electricity price.

**Fig. 4.** Input data for one possible scenario.

case, a residential MG that has a larger load would be tested. The input parameters and data of the simulation are derived for wind system from [34], for PV units from [35], for load from [36], and finally for energy prices from [37]. For example, data for solar power and wind generations, as well as prices and loads, are shown in Fig. 4 and b, respectively.

### 3.1. Determining the optimal capacity of the wind, solar, and battery simultaneously for an individual household

An individual home is considered as a small-scale electricity load, due to its low amount of energy consumption. The simulation data required in each step is presented in Table 1. The arrival time of the EV to the home is assumed to be at 19 o'clock and the time of departure from home is also set at 8 o'clock in the morning. It is also assumed that 60% of the home consumption is fixed and 40% of the remaining load is transferable from one period to another. Also, the maximum transferable capacity from each period to another period is assumed to be 1 kW. The price of electricity sales to the upstream network is also set at 0.50 $\$/kWh$. On the other hand, to increase the efficiency of the proposed model and to estimate the parameters with uncertainty, the effect of seasons and warm months of the year, and the change in the pattern of consumption in workdays and the weekends are considered. For this purpose, each year from the study period is divided into 12 monthly intervals, and then each month of the study is also modeled for four weeks and each week with five workdays and two weekends. This process enables the applicability of the proposed algorithm for use in real systems.

#### 3.1.1. Without development capability of HRES

In this section, the maximum allowable capacity for RESs and batteries is considered to be zero and the only smart controlling ability for the home is assumed. For each hour of the day, 10 different scenarios are used for load consumptions, as well as for electricity purchasing prices from the upstream network. The consumption scenarios and electricity prices for 24-hour horizon are shown in Fig. 5.

System operating costs by taking into account the costs and penalties associated with reducing household welfare (about 0.20 $\$/kWh$ for shifting from one period to another) in case of using demand response programs without using batteries and RESs becomes 31, 648.519$. Of course, this high value is due to the cost of interrupting and shifting the load, which is due to the reduction in welfare and is much higher than the normal price of electricity. However, the actual cost of subscribing is 1, 147.59$. This amount regardless of charging costs and only taking into account the cost of purchasing and selling electricity, and charging the EV seems reasonable. The charging and discharging of the EV for different scenarios, in one random sample day are depicted in Fig. 6. In these figures, first, the results of one scenario for both charging and discharging of the EVs, are illustrated and then figure for ten different scenarios are shown. The shape of the results and behavior of the system are analogous. For instance, when the electricity price is low, the EV is charged and the discharging process begins because of the higher price of electricity.

It is noteworthy to mention that in the simulations, employing demand response programs and energy storage capability of EVs is considered in the operation of a home. By neglecting these options, the operating costs become 61, 533.007$, which is far higher than the cost of the previous case.

#### 3.1.2. Considering expansion of renewable energy sources

In this case study, it is possible to take advantage of the output power of RESs, but at the moment, we assume that there is no battery. Therefore, the operation of determining the optimal capacity for two RESs of solar and wind will be done. In this regard, scenarios of wind and solar production will also be included in the issue. It should be kept in mind that the cost of investment and maintenance of RESs and the useful lifetime for these resources will have a significant impact on the optimization process, which will be considered and examined further. Four different conditions are considered and the input parameters for these conditions and optimization results are tabulated in Table 2. It is noteworthy to mention that the obtained results might be mathematical results and be far from commercial ratings; however, the nearest values can be chosen for the size of the components. For instance, the obtained result for the size of the wind unit is 19.2 $kW$ where a 20 $kW$ unit can be installed.

Four different conditions are considered in this case study. In the first case, it is assumed that the cost of investment and the cost of maintenance for a solar source is high compared to the source of wind and there is no limit for the capacity development of these resources. Thus, as can be seen from this table for the first mode, only wind turbines are used and it is not economically feasible to use PV units. In the second case, the development of these resources is limited, which results in reducing the wind turbine's optimal capacity. In the third case, the cost of investing and constructing RESs is less than the previous two. Again, given the wind capacity of the region, it is preferable to use maximum wind energy. In the fourth case, it is assumed that the development and construction of wind units are limited to 5 kW, but the capacity of the solar source can be expanded to 15 kW. In this new situation, which is evident in the fourth column, it can be seen that the wind unit is developed first, then a PV source is added, with an optimal capacity of 10 kW.

As discussed in the previous section, the cost of operating the system, regardless of the development capabilities, is 31, 448.188$. The operating cost of the system with capability developing RESs is reduced to 17, 984.845$ by taking into account the values of Table 2 for the development of the grid.

#### 3.1.3. Effect of developing energy storage devices alongside renewable energy sources

In this section, the effect of battery storage utilization alongside determining its optimal capacity is considered in the presence of RESs and demand response programs. In this case, all of the components are connected to the grid and the goal is to determine their optimal capacity. In this case, likewise the previous subsection, different situations may occur, and the results will be presented and examined. In the first case, there is no limit to the development of the capacity of RESs and a battery. The results of optimum planning of the system alongside with system parameters can be derived from Table 3. The amounts of the variables of the objective function can be seen in Fig. 7. The results in this form show the cost reduction and the significant profit generated by the optimal capacity determination.

As can be seen, in this case, costs have become negative, which is due to relaxing the constraints of developing the HRES. In this case, using large energy storage devices enables the owner to gain more

**Table 1**
Input parameters for solving the problem in an individual home.

| Input Parameter | Value |
|---|---|
| Planning period | 5 Years |
| Real interest rate | 5% |
| EV charging rate | 3.3 kW |
| EV discharge rate | 3.3 kW |
| EV capacity | 16 kWh |
| EV efficiency in charging mode | 90% |
| EV efficiency in discharging mode | 90% |
| Maximum EV energy level | 16 kWh |
| Minimum EV energy level | 2 kWh |
| Maximum battery energy level | 100% |
| Minimum battery energy level | 20% |
| Battery charging efficiency | 90% |
| Battery discharge efficiency | 90% |
| Maximum load of the home | 6 kWh |

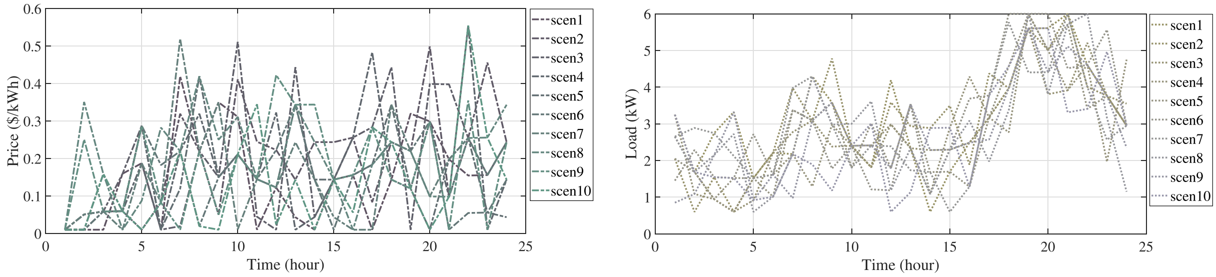


(a) Price scenarios for purchasing electricity.

(b) Consumption scenarios for loads of the home.

**Fig. 5.** Different scenarios for electricity price and load consumption.

profit by storing energy at times when the price of electricity is low and selling it to the network at times when the price is high. The *TC* variable is the difference between the cost of purchasing electricity and the revenue generated by electricity sales, which is 50, 000$ annually, which suggests that if there is no limit for the development of resource capacities and the smart usage of the battery system and renewable energy, it can benefit considerably. Battery charging and discharging performance for various scenarios for a random day in a sample year are shown in Fig. 8. In this case, due to freedom in the capacity of renewable-based energy sources, the flexibility of charging and discharging has risen in comparison with the system without expansion capability. However, the behavior for the charging and discharging is the same as charging in lower price hours and discharging in higher price periods.

In the second, the capacity for developing different sources are limited. Due to limitations on the maximum expandable capacity, the calculated values for the variables of the objective function also change. These variables are shown in Fig. 9. However, with limiting the capacity development, less profit than the ideal mode (first mode) is obtained. Also, the profit is still high compared to the case without taking advantage of the storage systems. As shown in Table 3 for the second mode, the maximum capacity of the battery is used considering the limitations and despite the high costs of investment and maintenance of PV systems, there is still considerable potential for their development. It seems to be feasible to allow the production of this resource throughout the day, at peak times and high price levels.

In this condition, the profit from the purchasing and selling the electricity is 26, 000$ a year, which is less than the amount of profit in the unconstrained state. To better illustrate the performance of the battery, similar to the previous subsection and the charging and discharging are shown for a sample day and various scenarios in Fig. 10. Although in comparison with the relaxed test system for expansion

**Table 2**
The optimal RESs development and data for the home with capability of only renewable source development.

| Case | Source | Investment cost ($/kW) | Maintenance cost ($/kW) | Maximum development capacity (kW) | Optimized capacity (kW) |
|---|---|---|---|---|---|
| 1 | Wind | 190 | 30 | Unlimited | 19.2 |
| | Solar | 1300 | 65 | Unlimited | 0 |
| 2 | Wind | 190 | 30 | 8 | 2.66 |
| | Solar | 1300 | 65 | 8 | 0 |
| 3 | Wind | 40 | 15 | Unlimited | 19.2 |
| | Solar | 60 | 10 | Unlimited | 0 |
| 4 | Wind | 40 | 15 | 5 | 5 |
| | Solar | 60 | 10 | 15 | 10.02 |

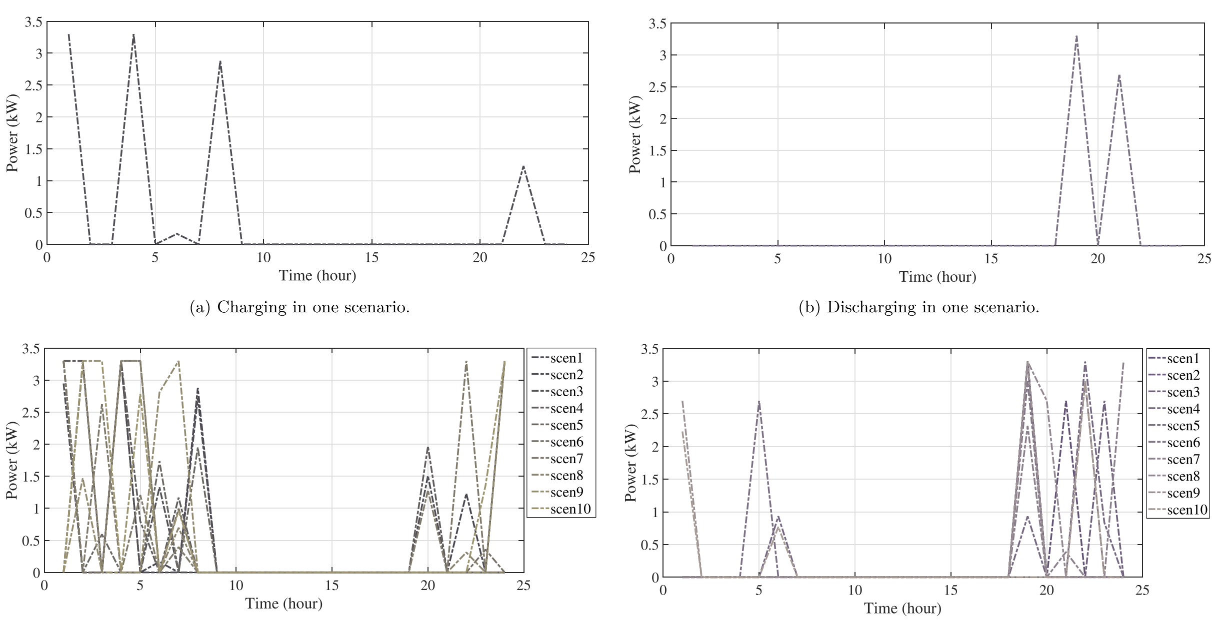


(a) Charging in one scenario.

(b) Discharging in one scenario.

(c) Charging in ten different scenarios.

(d) Discharging in ten different scenarios.

**Fig. 6.** Charging and discharging of the EV on January 1st for the home without developing capability.

**Table 3**
The optimal RESs and battery development and data for the home.

| Case | Source | Investment cost ($/kW) | Maintenance cost ($/kW) | Maximum development capacity | Optimized capacity |
|---|---|---|---|---|---|
| 1 | Wind | 190 | 45 | Unlimited | 24.4 kW |
| | Solar | 400 | 50 | Unlimited | 3.4 kW |
| | Battery | 250 | 40 | Unlimited | 50 kWh |
| 2 | Wind | 190 | 45 | 8 kW | 7 kW |
| | Solar | 400 | 50 | 10 kW | 9.25 kW |
| | Battery | 250 | 40 | 10 kWh | 10 kWh |
| 3 | Wind | 1200 | 90 | 10 kW | 2 kW |
| | Solar | 2000 | 130 | 10 kW | 0 kW |
| | Battery | 600 | 50 | 10 kWh | 5 kWh |

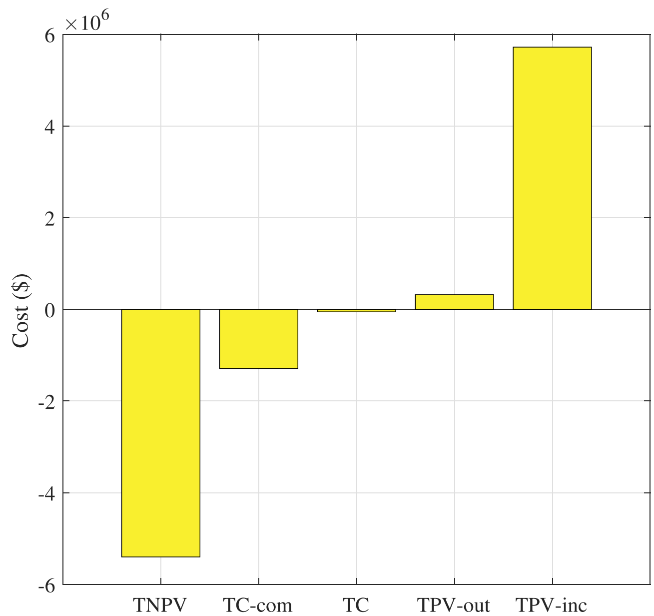


**Fig. 7.** Variables of the objective function for the home with development capability in the first condition.

capacity, in this case, the amount of the charging and discharging values are decreased, it shows more flexibility for charging and discharging rates compared to the system without expansion capability.

Also, in Fig. 11, the smart changes in the load are shown in one of the scenarios concerning electricity prices. Given the real-time price (Fig. 5) and the comparison of two subplots, the smart performance of the proposed method is clearly evident in the shifting of the load to periods at lower prices and at times that the price increases, the load is transmitted smartly to other times with lower price.

However, the calculated values for optimal resource development will be heavily dependent on the investment and maintenance costs of these resources. In order to confirm this hypothesis, in the third condition, higher costs are considered these sources and the optimal development of the HRES is made. Comparing the results of conditions 1 and 2, and the results of condition 3, it can be deduced that by reducing the cost of developing RESs in future years, it will be possible to increase the penetration of these resources and make MG development more efficient.

### 3.2. Determining the optimal capacity of the wind, solar, and battery simultaneously for larger MG

This section is dedicated to determining the optimum energy storage and RESs as PV systems and wind turbines capacity along with the use of demand response programs for a larger residential MG, which is composed of several residential partnerships. Considering the performance of the model entirely and with various details in the previous section, this stage only explores how to determine the optimal capacity of these resources for a large residential MG, and the appropriate amount for battery capacity, wind and PV resources is obtained.

The values assumed in this case for the load set are presented in Table 4. In this new situation, due to the constraints, the optimal capacity determination is obtained from the optimization process and the results are presented in Table 5. It is seen that in this case, with regard to the prices and constraints, it is preferable to use wind turbines and batteries. Also, the calculated values for the variables of the objective function are shown in Fig. 12. It should be noted that in this case, the network is under a heavy load, so the cost is high due to the sales and purchasing limit of the network (which is assumed to be 300 kW). Thus, it is not allowed to sell more power to the upstream network to gain

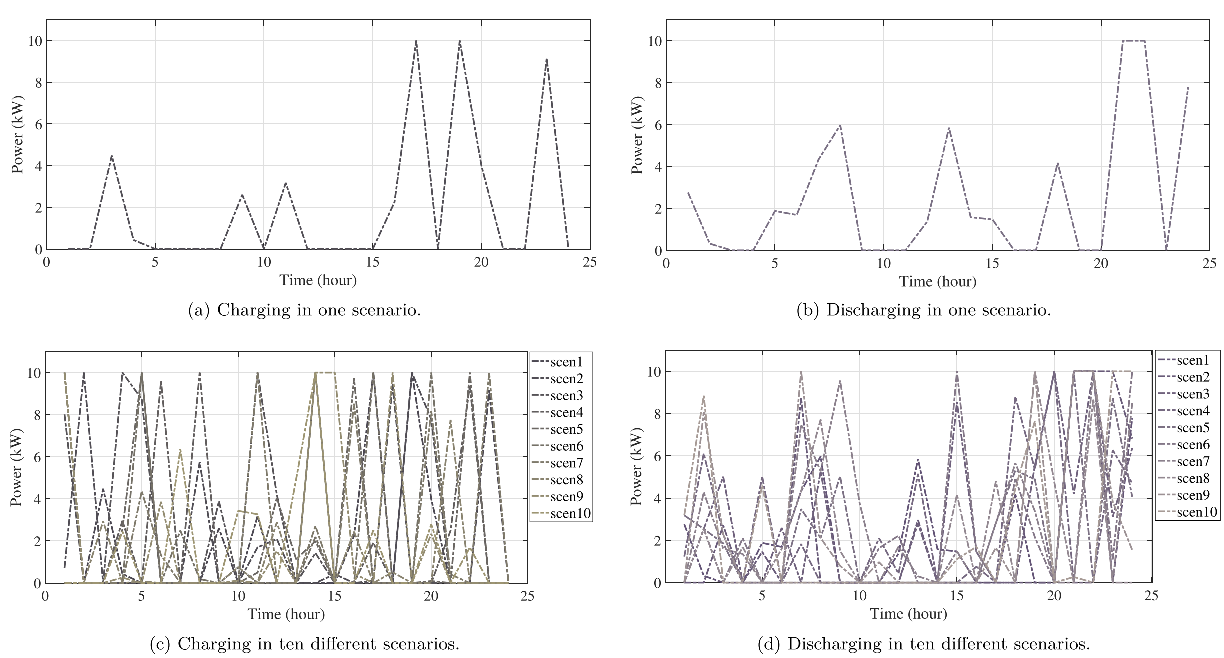


(a) Charging in one scenario.
(b) Discharging in one scenario.
(c) Charging in ten different scenarios.
(d) Discharging in ten different scenarios.

**Fig. 8.** Charging and discharging of the EV on January 1st for the home with development capability in the first condition.

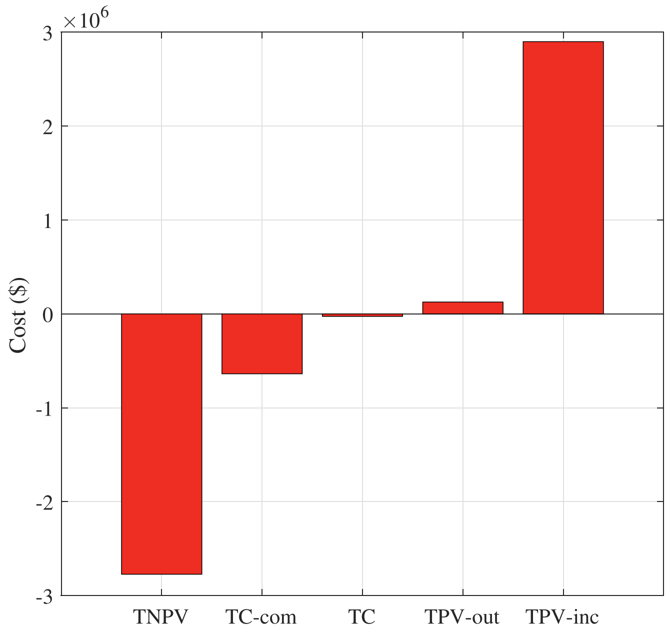


**Fig. 9.** Variables of the objective function for the home with development capability in the second condition.

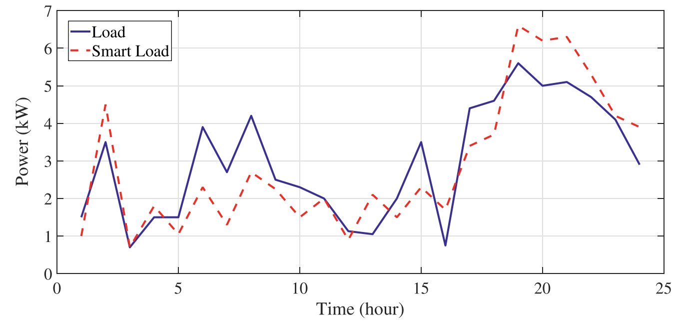


**Fig. 11.** Load curve with/without demand response programs.

**Table 4**
Input parameters for solving the problem in a larger MG.

| Input Parameter | Value |
|---|---|
| Planning period | 5 Years |
| Real interest rate | 5% |
| Integrated EV charging rate | 21 kW |
| Integrated EV discharge rate | 21 kW |
| Integrated EV capacity | 120 kWh |
| EV efficiency in charging mode | 90% |
| EV efficiency in discharging mode | 90% |
| Maximum EV energy level | 16 kWh |
| Minimum EV energy level | 2 kWh |
| Maximum battery energy level | 100% |
| Minimum battery energy level | 20% |
| Battery charging efficiency | 90% |
| Battery discharge efficiency | 90% |
| Integrated maximum load of the HRES | 300 kWh |
| Maximum power transactions with the upstteam network | 300 kW |

more profit, but with relaxing the limits of the transaction, more revenue will be available.

### 3.2.1. Deterministic MILP for determining the optimal capacity of the wind, solar, and battery simultaneously for larger MG

In this part, in order to have an overview of the comparison between the proposed stochastic MILP method and the deterministic MILP model, the deterministic approach has been applied to the planning problem. The results of the optimization are presented in Table 6. It can be seen in the deterministic model, unreal results are achieved and for instance, solar and wind units, the maximum available value has been selected, which may increase the investment costs. The costs are shown in Fig. 13. The operational costs have been increased in comparison with the proposed model. Furthermore, *TNPV* is higher than the stochastic approach. Accordingly, in the proposed stochastic model, the results are more realistic.

### 3.3. Utilized software information

All tests were run utilizing General Algebraic Modeling System (GAMS) and Matlab software on a Corei5 CPU 1.07 GHz computer with

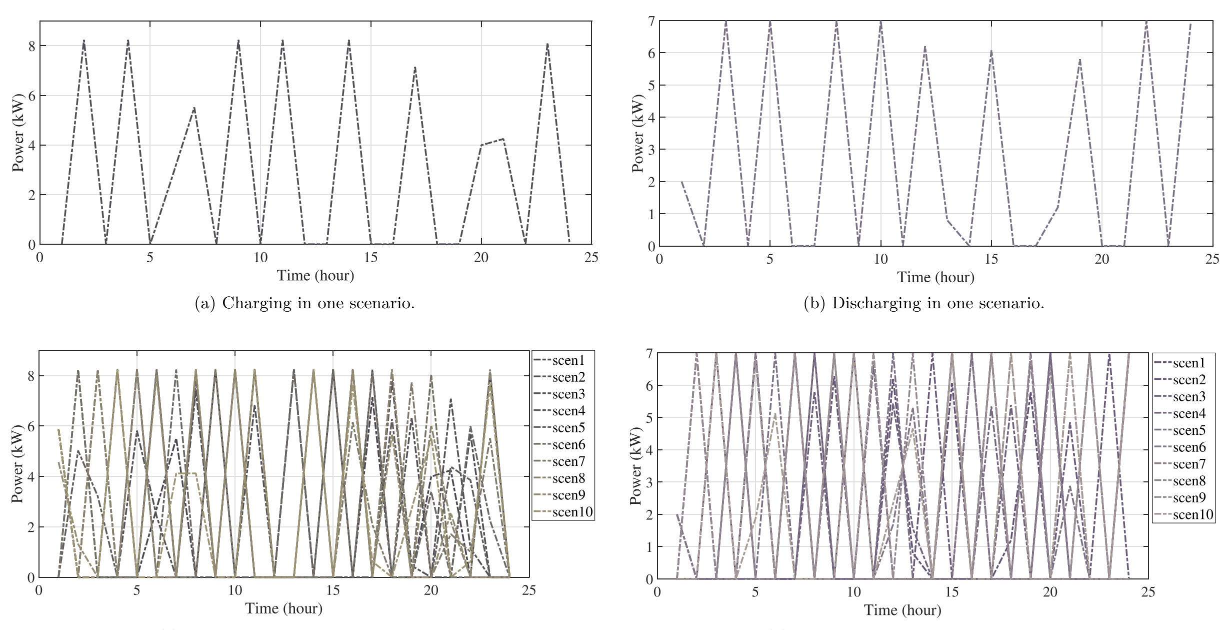


**Fig. 10.** Charging and discharging of the EV on January 1st for the home with development capability in the second condition.

**Table 5**
Optimal RESs and battery development and data, for a larger residential MG.

| Source | Investment cost ($/kW) | Maintenance cost ($/kW) | Maximum development capacity (kW) | Optimized capacity (kW) |
|---|---|---|---|---|
| Wind | 190 | 45 | 300 kW | 116 kW |
| Solar | 400 | 50 | 300 kW | 16.7 kW |
| Battery | 250 | 40 | 300 kW | 262 kW |

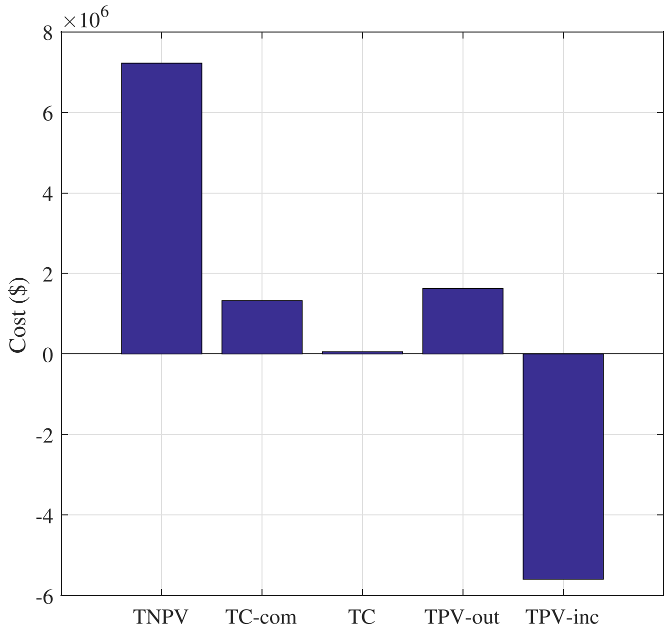


**Fig. 12.** Variables of the objective function for a residential MG.

**Table 6**
Optimal RESs and battery development and data, for a larger residential MG using deterministic MILP.

| Source | Investment cost ($/kW) | Maintenance cost ($/kW) | Maximum development capacity (kW) | Optimized capacity (kW) |
|---|---|---|---|---|
| Wind | 190 | 45 | 300 kW | 300 kW |
| Solar | 400 | 50 | 300 kW | 300 kW |
| Battery | 250 | 40 | 300 kW | 100 kW |

4 GB of RAM. The maximum run time was 16 min. For the micro-grid case, which is the biggest model, the number of single variables is 274, 664 along with 14, 800 discrete ones. Also, there are 51 blocks of equation, including 154, 187 single equations. Stopping criteria was set to $10^{-5}$ for all cases.

## 4. Conclusion

In this paper, a useful tool was proposed for residential MG designers to determine the optimal capacity of RESs and BESSs. Additionally, a grid operator can use this tool for optimal energy management in the system. The proposed resource development leads to a significant impact on reducing the cost of electricity supply needed by consumers. From the operator viewpoint, uncertainties shall be managed by using EVs connected to the MG, and meantime, considering different patterns of charging and discharging of EVs provides higher profitability. Also, employing demand response programs could increase the overall benefits gained by the owner of the system.

The proposed method showed its efficiency in dealing with a large-scale problem by applying the MILP approach and employing precise stochastic modeling for uncertainties. In future work, other methods for uncertainties modeling and robust optimization framework will be implemented.

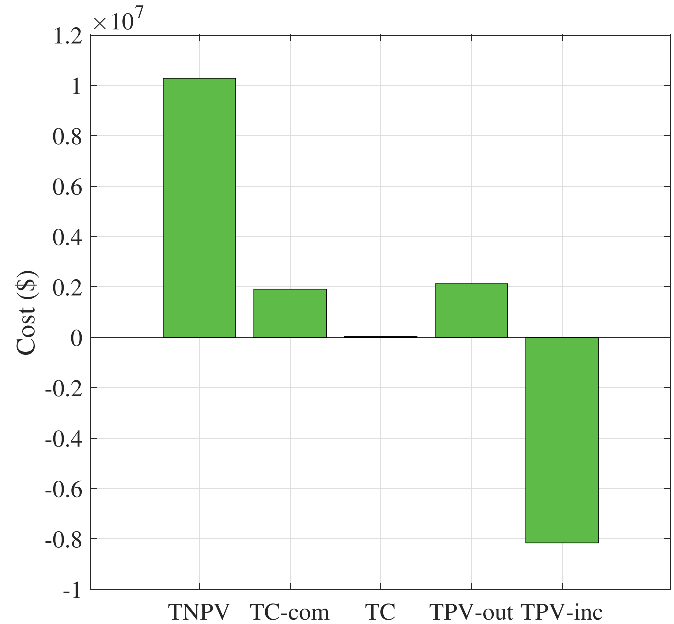


**Fig. 13.** Variables of the objective function for a residential MG in deterministic approach.

## CRediT authorship contribution statement

**Meisam Farrokhifar:** Supervision, Investigation, Conceptualization, Methodology, Validation, Formal analysis, Data curation, Writing - original draft, Writing - review & editing, Visualization. **Farid Hamzeh Aghdam:** Conceptualization, Methodology, Software, Validation, Formal analysis, Writing - original draft, Writing - review & editing, Visualization. **Arman Alahyari:** Conceptualization, Methodology, Software, Validation, Formal analysis, Data curation, Writing - original draft, Writing - review & editing, Visualization. **Ali Monavari:** Conceptualization, Methodology, Formal analysis, Software, Writing - review & editing, Visualization. **Amin Safari:** Conceptualization, Methodology, Formal analysis, Writing - review & editing, Visualization.

## Declaration of Competing Interest

All authors have participated in (a) conception and design, or analysis and interpretation of the data; (b) drafting the article or revising it critically for important intellectual content; and (c) approval of the final version. The authors have no affiliation with any organization with a direct or indirect financial interest in the subject matter discussed in the manuscript.

## References


[1] H. Park, R. Baldick, Optimal capacity planning of generation system integrating uncertain solar and wind energy with seasonal variability, Electr. Power Syst. Res. 180 (2020) 106072.
[2] B. Faridpak, A. Alahyari, M. Farrokhifar, H. Momeni, Toward small scale renewable energy hub-based hybrid fuel stations: appraising structure and scheduling, IEEE Trans. Transp. Electrif. 6 (1) (2020) 267–277.
[3] A. Foley, A.G. Olabi, Renewable energy technology developments, trends and policy implications that can underpin the drive for global climate change, Renew. Sustain. Energy Rev. 68 (2017) 1112–1114.
[4] M. Farrokhifar, S.M. Mahaei, J. Jafarzadeh, M. Gholami, Distribution networks reconfiguration for loss minimization based on variable behavior of loads and energy cost curves, 39th Annual Conference of the IEEE Industrial Electronics Society, (2013), pp. 2022–2026.
[5] O. Hafez, K. Bhattacharya, Optimal planning and design of a renewable energy

based supply system for microgrids, Renew. Energy 45 (2012) 7–15.
[6] A. Safari, F. Babaei, M. Farrokhifar, A load frequency control using a PSO-based ANN for micro-grids in the presence of electric vehicles, Int. J. Ambient Energy (2019) 1–13.
[7] O. Nadjemi, T. Nacer, A. Hamidat, H. Salhi, Optimal hybrid PV/wind energy system sizing: application of cuckoo search algorithm for Algerian dairy farms, Renew. Sustain. Energy Rev. 70 (2017) 1352–1365.
[8] R. Atia, N. Yamada, Sizing and analysis of renewable energy and battery systems in residential microgrids, IEEE Trans. Smart Grid 7 (3) (2016) 1204–1213.
[9] M. Gomez-Gonzalez, J.C. Hernández, D. Vera, F. Jurado, Optimal sizing and power schedule in PV household-prosumers for improving PV self-consumption and providing frequency containment reserve, Energy 191 (2020) 116554.
[10] H. Bakhshi Yamchi, H. Shahsavari, N. Taghizadegan Kalantari, A. Safari, M. Farrokhifar, A cost-efficient application of different battery energy storage technologies in microgrids considering load uncertainty, J. Energy Storage (2019) 17–26.
[11] J.C. Hernández, F. Sanchez-Sutil, F.J. Muñoz-Rodríguez, Design criteria for the optimal sizing of a hybrid energy storage system in PV household-prosumers to maximize self-consumption and self-sufficiency, Energy 186 (2019) 115827.
[12] M. Farrokhifar, Optimal operation of energy storage devices with RESs to improve efficiency of distribution grids; technical and economical assessment, Int. J. Electr. PowerEnergy Syst. 74 (2016) 153–161.
[13] H.F. Gharibeh, L.M. Khiavi, M. Farrokhifar, D. Pozo, Life cycle cost analysis of electric vehicles based on critical price and critical distance, IEEE PES Innovative Smart Grid Technologies Europe (ISGT-Europe), (2019), pp. 1–5.
[14] J.C. Hernández, F.J. Ruiz-Rodriguez, F. Jurado, Modelling and assessment of the combined technical impact of electric vehicles and photovoltaic generation in radial distribution systems, Energy 141 (2017) 316–332.
[15] N. Neyestani, M.Y. Damavandi, M. Shafie-Khah, J. Contreras, J.P. Catalão, Allocation of plug-in vehicles' parking lots in distribution systems considering network-constrained objectives, IEEE Trans. Power Syst. 30 (5) (2015) 2643–2656.
[16] F.J. Ruiz-Rodriguez, J.C. Hernández, F. Jurado, Voltage behaviour in radial distribution systems under the uncertainties of photovoltaic systems and electric vehicle charging loads, Int. Trans. Electr. Energy Syst. 28 (2) (2018) e2490.
[17] B. Faridpak, H.F. Gharibeh, M. Farrokhifar, D. Pozo, Two-step LP approach for optimal placement and operation of EV charging stations, IEEE PES Innovative Smart Grid Technologies Europe (ISGT-Europe), (2019), pp. 1–5.
[18] J.-M. Clairand, M. Arriaga, C.A. Canizares, C. Alvarez, Power generation planning of Galapagos' microgrid considering electric vehicles and induction stoves, IEEE Trans. Sustain. Energy 10 (4) (2019) 1916–1926.
[19] T. Alharbi, K. Bhattacharya, M. Kazerani, Planning and operation of isolated microgrids based on repurposed electric vehicle batteries, IEEE Trans. Ind. Inf. 15 (7) (2019) 4319–4331.
[20] M. Moradijoz, M.P. Moghaddam, M.-R. Haghifam, A flexible distribution system expansion planning model: a dynamic bi-level approach, IEEE Trans. Smart Grid 9 (6) (2018) 5867–5877.
[21] M. ElNozahy, T.K. Abdel-Galil, M. Salama, Probabilistic ESS sizing and scheduling for improved integration of PHEVs and PV systems in residential distribution systems, Electr. Power Syst. Res. 125 (2015) 55–66.
[22] B. Zeng, J. Zhang, X. Yang, J. Wang, J. Dong, Y. Zhang, Integrated planning for transition to low-carbon distribution system with renewable energy generation and demand response, IEEE Trans. Power Syst. 29 (3) (2014) 1153–1165.
[23] X. Cao, J. Wang, B. Zeng, A chance constrained information-gap decision model for multi-period microgrid planning, IEEE Trans. Power Syst. 33 (3) (2018) 2684–2695.
[24] G. Mokryani, Active distribution networks planning with integration of demand response, Sol. Energy 122 (2015) 1362–1370.
[25] S. Bandyopadhyay, G.R. Chandra Mouli, Z. Qin, L.R. Elizondo, P. Bauer, Techno-economical model based optimal sizing of PV-battery systems for microgrids, IEEE Transactions on Sustainable Energy (2019). 1–1
[26] C. Gouveia, J. Moreira, C. Moreira, J.P. Lopes, Coordinating storage and demand response for microgrid emergency operation, IEEE Trans. Smart Grid 4 (4) (2013) 1898–1908.
[27] X. Xu, J. Mitra, N. Cai, L. Mou, Planning of reliable microgrids in the presence of random and catastrophic events, Int. Trans. Electr. Energy Syst. 24 (8) (2014) 1151–1167.
[28] S. Cano-Andrade, M.R. von Spakovsky, A. Fuentes, C.L. Prete, B.F. Hobbs, L. Mili, Multi-objective optimization for the sustainable-resilient synthesis/design/operation of a power network coupled to distributed power producers via microgrids, International Mechanical Engineering Congress and Exposition, American Society of Mechanical Engineers, 2012, pp. 1393–1408.
[29] A.K. Basu, S. Chowdhury, S. Chowdhury, Impact of strategic deployment of CHP-based DERs on microgrid reliability, IEEE Trans. Power Deliv. 25 (3) (2010) 1697–1705.
[30] X. Yang, W. Tian, Microgrid's generation expansion planning considering lower carbon economy, Asia-Pacific Power and Energy Engineering Conference (APPEEC), (2012), pp. 1–6.
[31] L. Guo, W. Liu, J. Cai, B. Hong, C. Wang, A two-stage optimal planning and design method for combined cooling, heat and power microgrid system, Energy Convers. Manage. 74 (2013) 433–445.
[32] A. Arif, Z. Wang, Service restoration in resilient power distribution systems with networked microgrid, Power and Energy Society General Meeting (PESGM), 2016, IEEE, 2016, pp. 1–5.
[33] S. Rahmani, N. Amjady, A new optimal power flow approach for wind energy integrated power systems, Energy 134 (2017) 349–359.
[34] Wind-power generation data, 2018, http://www.elia.be/en/grid-data/power-generation/wind-power.
[35] Solar power data for integration studies, 2018, https://www.nrel.gov/grid/solar-power-data.html.
[36] Historical EMS hourly load data available, 2018, http://www.caiso.com/planning/Pages/ReliabilityRequirements/Default.aspx#Historical.
[37] Real time hourly prices., 2018, https://hourlypricing.comed.com/live-prices/.